Phosphorylation of the C-Terminal Sites of Human p53 Reduces Non-Sequence-Specific DNA Binding as Modeled with Synthetic Peptides[†]

Ralf Hoffmann,[‡] David J. Craik,[§] Greg Pierens,[||] Randall E. Bolger,[⊥] and Laszlo Otvos, Jr.*[,‡]

The Wistar Institute, 3601 Spruce Street, Philadelphia, Pennsylvania 19104, Centre for Drug Design and Development, The University of Queensland, Brisbane, Australia, Queensland Pharmaceutical Research Institute, Griffith University, Nathan, Australia, and PanVera Corporation, Madison, Wisconsin 53711

Received April 3, 1998; Revised Manuscript Received June 24, 1998

ABSTRACT: Phosphorylation of the tumor suppressor p53 is generally thought to modify the properties of the protein in four of its five independent domains. We used synthetic peptides to directly study the effects of phosphorylation on the non-sequence-specific DNA binding and conformation of the C-terminal, basic domain. The peptides corresponded to amino acids 361−393 and were either nonphosphorylated or phosphorylated at the protein kinase C (PKC) site, Ser378, or the casein kinase II (CKII) site, Ser392, or bis-phosphorylated on both the PKC and the CKII sites. A fluorescence polarization analysis revealed that either the recombinant p53 protein or the synthetic peptides bound to two unrelated target DNA fragments. Phosphorylation of the peptide at the PKC or the CKII sites clearly decreased DNA binding, and addition of a second phosphate group almost completely abolished binding. Circular dichroism spectroscopy showed that the peptides assumed identical unordered structures in aqueous solutions. The unmodified peptide, unlike the Ser378 phosphorylated peptide, changed conformation in the presence of DNA. The inherent ability of the peptides to form an α-helix could be detected when circular dichroism and nuclear magnetic resonance spectra were taken in trifluoroethanol−water mixtures. A single or double phosphorylation destabilized the helix around the phosphorylated Ser378 residue but stabilized the helix downstream in the sequence.

Tumor suppressor protein p53 is considered a guardian of the genome (*1*). The p53 gene encodes a nuclear phosphoprotein that is altered by mutation or deletion in about 50% of human tumors (*2*). p53 was first reported to be an oncogene (*3, 4*), but later wild-type p53 was recognized as a negative growth regulator or tumor suppressor gene (*5*). The p53 protein can be and usually is divided into four (*6*) or five (*7*) distinct regions (Figure 1). The transactivation domain is found in the first 42 amino acid stretch. This region mediates the transcriptional activity of p53,[1] which is directly correlated to its ability to suppress cell growth (*8*). The next, recently characterized domain, amino acids 61−94, is responsible for growth suppression (*7*). The so-called DNA-binding domain, located between amino acids 96 and 286, is responsible for sequence-specific DNA binding (*9*). The tetramerization domain, amino acids 319−360, of p53 interacts with other p53 protein chains to build a more active tetramer, as is shown by peptide mapping (*10*). In reality this is not a true tetramer, but a dimer of dimers in which each chain contributes with a β-pleated sheet and an α-helix (*11, 12*). The fifth, the basic, domain is highly positively charged and therefore interacts non-sequence specifically with DNA (i.e., binds to many DNA sequences).

The basic domain is located at the C-terminal region between amino acids 363 and 386 (*13, 14*), although this domain is often considered to stretch out until the end of the protein molecule (amino acids 363−393). When p53 lacks the last 30 amino acids at the C-terminal end, it exhibits higher double-stranded DNA affinity, suggesting a negative regulation of specific DNA binding by the basic region (*15, 16*), but this same truncation activates binding to damaged DNA structures (*17, 18*).

Phosphorylated serines and threonines span the entire p53 protein, and distinct phosphorylation sites are found in at least three domains and in the flexible segments between them (Figure 1). It seems that the N-terminal and the C-terminal regions are the major sites of protein kinase activity. At the C-terminal region, protein kinase C (PKC)[2] can phosphorylate p53 in vitro and in vivo (*19*). Only phosphorylation of Ser378 has been identified so far by PKC (*20*) although, based on the consensus sequences for this kinase, four additional target residues are located in the basic region of p53 (Ser367, Ser371, Ser376, and Thr377) (*19*).

[†] This work was partially funded by the NIH Grant GM 55860 (L.O.).

* Corresponding author: telephone, (215) 898-3772; fax, (215) 898-5821; e-mail, otvos@wista.wistar.upenn.edu; institute URL, http://www.wistar.upenn.edu.

[‡] The Wistar Institute.

[§] Centre for Drug Design and Development.

[||] Queensland Pharmaceutical Research Institute.

[⊥] PanVera Corporation.

[1] Please note that all amino acid numbering corresponds to the human p53 sequence. If the original publications use homologous sequences from mutants or other species the numbering is "translated" to the appropriate human p53 positions.

[2] Abbreviations: PKC, protein kinase C; CKII, casein kinase II; RP, reversed-phase; CD, circular dichroism; NMR, nuclear magnetic resonance.

S0006-2960(98)00760-0 CCC: $15.00
Published on Web 09/05/1998

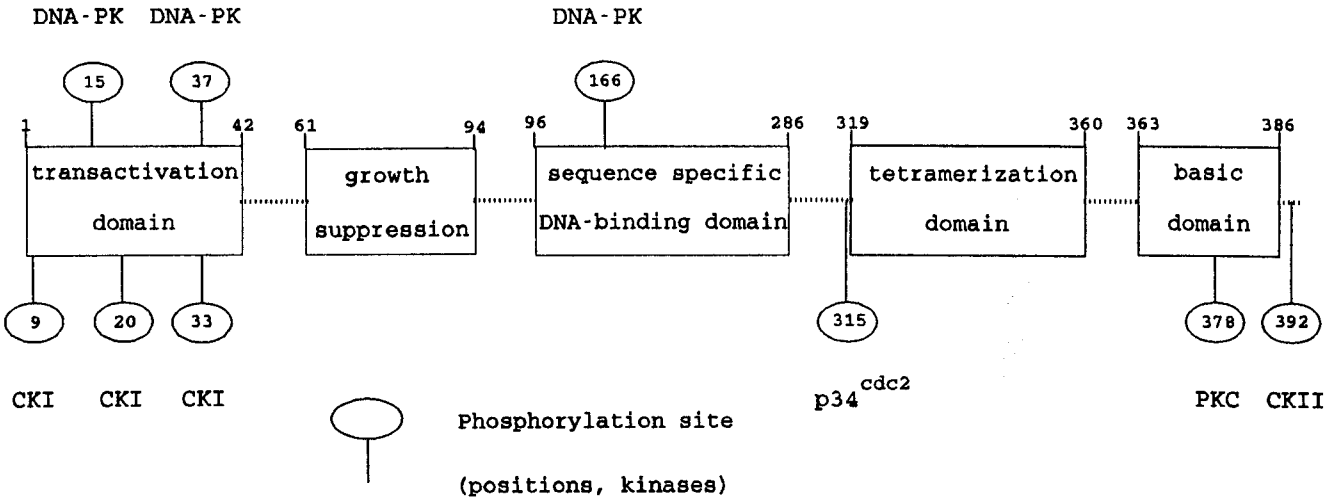

FIGURE 1: Five-domain structure of p53 protein. The numerals in ellipses show the positions of established phosphorylation sites (all serines) in vivo or in vitro. The kinases which can phosphorylate the indicated positions of p53 are shown above or below the ellipses.

Table 1: Synthetic Peptides and Their Characterization

peptide[a]	sequence[b]	retention time on RP-HPLC (min)	MALDI mass spectru [M + H$^+$] (Da)
p53 361−393 nP	GSRAHSSHLKSKKGQST**S**RHKKLMFKTEGPD**S**D	23.4	3655
p53 378P	**S***	23.4	3736
p53 392P	**S***	23.4[c]	3736
p53 378P, 392P	**S*** **S***	23.9	3819
τ 390−408 nP	AEIVYKSPVV**S**GD**T**SPRHL	25.5	2055
τ 400 P	**S***	24.9	2134
τ 400P, 403P	**S*** **T***	25.3	2215

[a] nP = nonphosphorylated peptide. [b] Amino acids marked with asterisks indicate the position of phosphorylation. [c] Measured on a somewhat slower eluting column.

Phosphorylation of p53 by PKC activates DNA binding, and the binding can be reversed by protein phosphatases 1 and 2A (*20*). Casein kinase II (CKII) can phosphorylate Ser392, the penultimate residue, located just beyond the basic domain (*21*, *22*). Phosphorylation of the C-terminal sites appears to promote sequence-specific DNA binding; however it also appears to de-activate non-sequence-specific DNA binding.

In the current study, we analyzed the effects of phosphorylation on two of the most widely studied properties of the C-terminal, basic domain of p53. We investigated direct DNA binding and conformation in solvent environments proven to be useful for the appropriate studies. To overcome the bias introduced by specific cell lines and the expression of mutated proteins, well-characterized synthetic model peptides and phosphopeptides were used in cell-free systems (Table 1). The domain structure of p53 allows the use of synthetic peptides to model the main features of function and structure of a given region of the protein.

MATERIALS AND METHODS

Peptide Synthesis. Peptides were synthesized on a Milligen 9050 automatic synthesizer using 9-fluorenylmethoxycarbonyl amino acids according to standard procedures (*23*). Phosphoserine residues were incorporated as Fmoc-Ser(PO_3HBzl)-OH (*24*), purchased from Novabiochem, Ltd. (San Diego, CA). Peptides and phosphopeptides were detached from the solid support with trifluoroacetic acid, and they were purified by reversed-phase (RP)-HPLC using an aqueous acetonitrile gradient elution system containing 0.1% trifluoroacetic acid as an ion-pairing reagent. The integrity of the peptides and phosphopeptides was verified by mass spectroscopy. Table 1 lists the synthetic peptides.

Control p53 Protein. Recombinant p53 cDNAs were cloned into the bacterial expression vector pT5T encoding an additional N-terminal 6-histidine epitope tag. Recombinant proteins were expressed in *Escherichia coli* BL21. Bacteria were lysed in an extraction buffer, and bacterial DNA was degraded by addition of 50 mg/mL of DNase I. The suspension was cleared by centrifugation at 120000*g* at 4 °C, and p53 protein in the supernatant was purified over a metal-chelating column (Pharmacia, Piscataway, NJ) according to the instructions of the manufacturer. This p53 preparation was used as a positive control for non-sequence-specific DNA binding. Bacterial environments for phosphorylation usually lack eukaryotic kinases. This frequently prevents proper phosphorylation from occurring (*25*). Thus, p53 produced in *E. coli* is likely to be unphosphorylated or phosphorylated at a low level.

DNA Binding. The ability of the peptides to bind DNA was assessed by fluorescence polarization (*26*). To this end, two fluorescein-labeled oligonucleotide probes were used (Table 2). The first was a 25-base oligonucleotide (F-trpO) from the trp operator sequence (*27*), and the second (F-BC-CB) was reported to bind to the sequence-specific DNA-binding domain of p53 (*16*). Although both oligonucleotide probes can form hairpin loop structures or homodimer double-stranded DNA, on the basis of secondary structure prediction, the formation of hairpins is favored only for the BC-CB sequence and not for the trpO sequence. The use

Table 2: Fluorescein-Labeled Oligonucleotides used for the DNA Binding Studies[a]

F-trpO	5′	Fluorescein-ATCGAACTAGTTAACTAGTACGCAA	3′
F-BC-CB	5′	Fluorescein-TTAAGGACATGCCCGGGCATGTCC	3′

[a] For CD, BC-CB was used without the addition of a fluorescein label.

of the F-trpO oligonucleotide as a probe for non-sequence-specific DNA binding of the p53 peptides is further justified by the extensive use of this labeled oligonucleotide as a probe for fluorescence polarization studies (*27*). Fluorescein was coupled to the 5′ end of the oligonucleotides by using a cyanoethyl protected phosphoramidite reagent containing a 6-carbon spacer arm between the phosphate group and the 6-carboxy group of the fluorescein. While fluorescein−phosphoramidites with longer spacer arms are also available for certain applications, shorter arms are more suitable for fluorescence polarization because of the higher shift of polarization upon binding. The fluorescein-labeled oligonucleotides were purified by RP-HPLC on C_{18} columns. The labeled oligonucleotides showed single bands on denaturing polyacrylamide gel electrophoresis (20% polyacrylamide, 7 M urea), indicating complete fluorescein incorporation. Eight-tenths of 2 nM F-trpO or F-BC-CB was dissolved in phosphate-buffered saline, pH 7.4, and peptides (0.06−64 mM) or control recombinant p53 protein (200−400 nM) was added. The solvent was a simplified version of that generally used for protein-binding studies of F-trpO during fluorescence polarization analysis (*27*). The extent of fluorescence anisotropy was measured on a Beacon 2000 fluorescence polarization instrument (PanVera, Madison, WI) and calculated as millipolarization values, as is generally done in the literature. The filters used were 485 nm excitation and 535 nm emission with 3 nm bandwidth. The oligonucleotides were made by the Wistar Institute Oligonucleotide Facility, at Clonetech Laboratories (Palo Alto, CA) or purchased from Cruachem, Inc. (Dulles, VA). Curve fitting for Figure 3 was done by using a dose−response logistical transition and the Levenberg−Marquardt Algorithm within the SlideWrite software package.

CD. CD spectra were taken on a Jasco J720 instrument at room temperature in a 0.2 mm path length cell. Doubly distilled water and spectroscopy grade trifluoroethanol were used as solvents. The p53 peptide concentrations were about 0.5 mg/mL (approximately 130 mM), determined each time by quantitative RP-HPLC (*28*). The accuracy of this concentration determination for the p53 peptides was measured to be over 99%. Curves were smoothed by the algorithm provided by Jasco. Mean residue ellipticity ($[\Theta]_{MR}$) is expressed in deg·cm^2/dmol by using mean residue masses of 110.7, 113.2, and 115.7 Da, respectively, based on the actual molecular mass of the peptides. Because the secondary structures of the peptides (especially phosphopeptides) provided by the current computer-assisted curve-analyzing algorithms show a high error rate, the CD spectra evaluations were based on comparison with known peptide conformations (*29*, *30*). When the effect of the presence of the BC-CB oligonucleotide to the CD spectra of the p53 peptides was studied, the spectra were recorded in a buffer similar to the one in which positive binding of this DNA to the p53 protein was observed by gel mobility shift analysis (*16*). The solvent containing 25 mM Hepes, pH 7.4, and 50 mM KCl was transparent to the ultraviolet light and had manageable CD noise above 185 nm. For these experiments, the CD of the BC-CB oligonucleotide was independently recorded and digitally subtracted from the spectra of the peptide−oligonucleotide mixtures.

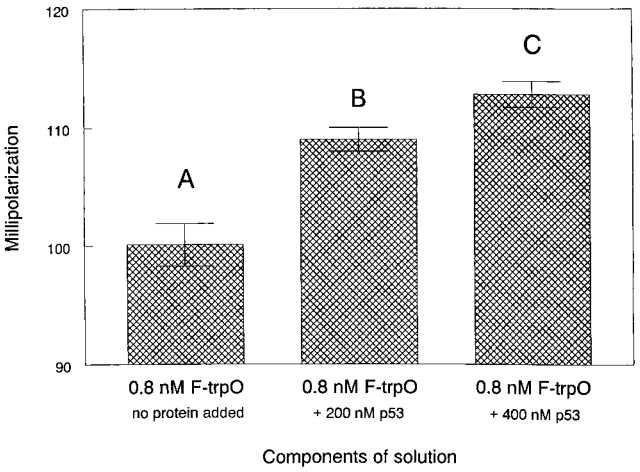

FIGURE 2: Binding of F-trpO oligonucleotide to p53 protein. (A) DNA (0.8 nM) without protein; (B) 0.8 nM DNA + 200 nM p53; (C) 0.8 nM DNA + 400 nM p53. The error bars indicate the standard deviations of five measurements. The experiments were performed at 22 °C.

Nuclear Magnetic Resonance (NMR). The ^{1}H NMR spectra were recorded for peptide p53 361−393 and its Ser378 phosphorylated analogue (1 mg in 550 mL of 50% d_3-trifluoroethanol−50% H_2O) on a Varian Unity Inova 600 MHz spectrometer at 10 °C, referenced to internal sodium 2,2-dimethyl-2-silapentene-5-sulfonate. ^{1}H NOESY 2D spectra were acquired with the following parameters: relaxation delay 2.0 s, mixing time 250 ms, number of points 4096, number of transients 64, acquisition time 0.3 s, spectral width 6856 Hz, and 512 increments in F_1 using phase-sensitive hypercomplex quadrature detection. The ^{1}H TOCSY 2D spectra were acquired under similar conditions with a mixing time of 80 ms. Water suppression was achieved by WATERGATE (using 3-9-19 pulses). A shifted sine-squared function was used as a weighting function in both F_1 and F_2 dimensions. Additional one-dimensional and TOCSY 2D spectra were acquired in 70%, 80%, 90%, and 100% trifluoroethanol−water mixtures.

RESULTS

DNA Binding. Recombinant p53 protein (expressed in *E. coli*) bound to both fluorescein-labeled oligonucleotides trpO and BC-CB (Table 2; details are found in Materials and Methods) in a protein concentration-dependent manner. Figure 2 shows the polarization shifts of F-trpO upon p53 binding. Considerable increase in the polarization of approximately 1 nM labeled oligonucleotide was detected after addition of p53 protein in a concentration as low as 200 nM. The extent of the shifts (9 millipolarization units) was almost identical for oligonucleotide F-BC-CB upon binding to the recombinant p53 protein (data not shown). When peptides (final concentration was 2.5 mM) were added to a 400 nM

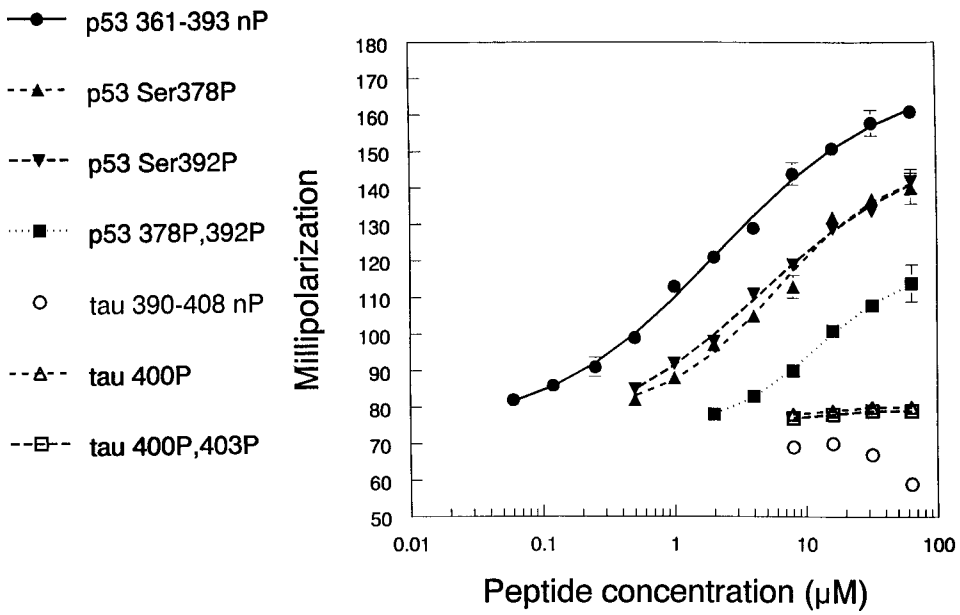

FIGURE 3: Binding of p53 peptides to F-trpO oligonucleotide. The peptides are shown in the legend and in Table 1. The fluorescence polarization (in millipolarization units) of the labeled trpO oligonucleotide without added peptide was 81.5 ± 0.5. The lower baseline value compared to lane A of Figure 2 is due to a higher incubation temperature. For these experiments, peptides were serially diluted in phosphate-buffered saline (pH 7.4) from 64 to 0.06 mM in a 100 mL final volume in a 6 × 50 mm disposable glass borosilicate tube. The F-trpO oligonucleotide probe was added to each tube in a 5-mL aliquot to a concentration of 2 nM, and tubes were incubated at 37 °C for 30 min. The error bars indicate the standard deviations of three replicate dilution series (five readings per data point for each sample). Nonlinear curve fitting was done by using a dose−response logistical transition [$y = a_0 + a_1/(1 + x/a_2)^{a3}$)] and the Levenberg−Marquardt Algorithm within the SlideWrite software package. The provided K_d values (a_2 coefficients: nonphosphorylated peptide, 2.1; Ser378P, 6.1; Ser392P, 4.6; bis-phosphorylated peptide, 12.0) were calculated by the program. Three independent series of dilutions and experiments yielded basically identical results.

p53 solution, a reduction in the polarization of the p53-specific BC-CB oligonucleotide was observed indicating that the peptides competed with the full protein for DNA binding. A decrease in the polarization was observed because the peptides with lower molecular masses bound competitively to the DNA to some extent, but the strength of the polarization signal was dependent upon the molecular mass of the binding partners. Direct peptide binding to 2 nM F-trpO or F-BC-CB DNA fragments was studied in the 0.06−64 mM peptide concentration range. The trpO sequence was selected over the BC-CB oligonucleotide for detailed analysis, because our preliminary results showed a higher degree of polarization shift with the trpO DNA than with the BC-CB upon binding to all four synthetic p53 peptides. At 64 mM of the best binder nonphosphorylated peptide, the polarization shift was 80 millipolarization units when mixed with 2 nM F-trpO and only 25 millipolarization units when mixed with 2 nM F-BC-CB. This was probably due to the presence of the 5′ four-base overhang of the BC-CB DNA which imparted significant mobility to fluorescein even when bound to the peptides. The overhang of F-BC-CB also explains the lower millipolarization value without addition of any binding partner. Nevertheless, the relative binding affinities of the four peptides to the two oligonucleotides were very similar. For negative controls, we used a peptide fragment corresponding to the low molecular mass microtubule-associated protein τ in nonphosphorylated, singly phosphorylated, and bis-phosphorylated forms (Table 1). At low peptide concentrations, none of the four p53 peptides bound notably to the F-trpO DNA. At higher concentrations, considerable binding of the nonphosphorylated peptide was observed (Figure 3). A clear-cut reduction in the DNA binding was found for the peptide phosphorylated at Ser378, the PKC site, or Ser392, the CKII site. Interestingly, the two singly phosphorylated peptides bound to the trpO oligonucleotide to an almost identical degree. The addition of the second phosphate group further reduced the ability of the peptides to bind DNA. The different abilities of the peptides to bind to the trpO oligonucleotide are well-documented in the increase of K_d values as the phosphate groups were added: nonphosphorylated p53, 2.1 mM; Ser378P, 6.1 mM; Ser392P, 4.6 mM; bis-phosphorylated p53, 12.0 mM. Nevertheless, even the doubly phosphorylated peptide bound to the trpO DNA above the control nonphosphorylated or phosphorylated τ peptides. It needs to be mentioned that higher polarization values were accompanied by higher variability of the readings. However, the reproducibility of three independent measurements of the same dilutions was always within a 5% error range. In yet another set of control experiments, addition of the p53 peptides to an N-terminally fluorescein-coupled peptide nucleic acid did not result in any polarization shift (data not shown), indicating that it is the negatively charged phosphate backbone and not the nucleobases that the positively charged peptides bind to.

As short peptides have extremely flexible termini and phosphorylation of Ser392, the penultimate residue, is not expected to modify the conformation of the p53 361−393 peptide alone, detailed CD and NMR analyses were performed only on the nonphosphorylated, Ser378 phosphorylated, and bis-phosphorylated peptide variants.

CD. CD studies of the p53 peptides in trifluoroethanol solutions were done to obtain information on the general effect of phosphorylation on the secondary structure of this flexible peptide. All three peptides exhibited similar mixtures of type U and type C spectra in 50% trifluoroethanol,

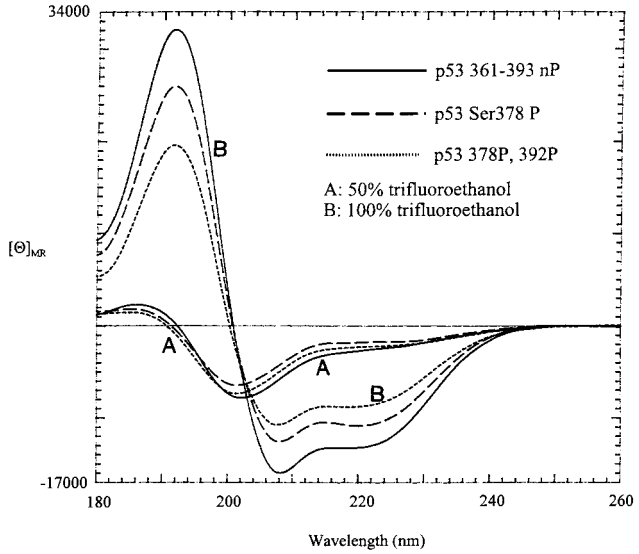

FIGURE 4: CD spectra of p53 peptides in 50% aqueous trifluoroethanol (A curves) and in 100% trifluoroethanol (B curves): solid traces, nonphosphorylated peptide; dashes, Ser378 phosphorylated peptide; dots, Ser378, Ser392 bis-phosphorylated peptide.

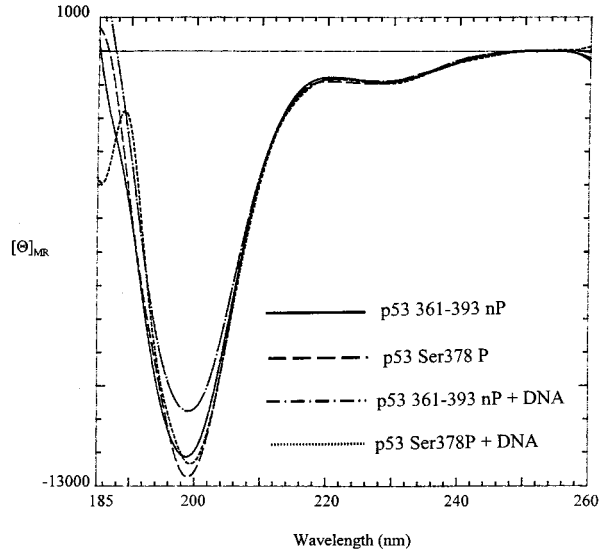

FIGURE 5: CD spectra of the nonphosphorylated peptide and the Ser378 phosphorylated peptide in the presence or absence of the 24-base oligonucleotide BC-CB. The spectra for p53 nP and p53 378P C-terminal peptides at concentrations of about 0.5 mg/mL (0.13 mM) were obtained in Hepes−KCl buffer (see Materials and Methods) without DNA and with equimolar DNA added. The control spectrum of the DNA alone was digitally subtracted from the spectra of the peptide−DNA mixtures.

indicating the presence of unordered structures and reversed turns (Figure 4). While the nonphosphorylated peptide possessed some α-helical character (6%), the Ser378 phosphorylated and the bis-phosphorylated peptides were essentially nonhelical (1% and 3% α-helix content, respectively). In 100% trifluoroethanol the unmodified peptide became fairly helical, the calculated α-helicity at 208 nm (*31*) reaching 41%. Phosphorylation at Ser378 destabilized the helix and reduced the α-helix content to 29%. The main conformational change could already be detected upon addition of the first phosphate group, and as expected, addition of the second phosphate to Ser392 decreased the α-helix content only slightly further (to 23%). We studied the relationship between peptide conformation and non-sequence-specific DNA binding. After learning that the peptides assume some ordered conformation in 50% trifluoroethanol, we repeated the fluorescence polarization assay with the three peptides and the F-trpO oligonucleotide in a trifluoroethanol−PBS = 1:1 (v/v) mixture in the 4−128 mM peptide concentration range (the CD studies were run at approximately 130 mM). Trifluoroethanol is known to decrease the dielectric constant of aqueous solutions. Because the binding of the cationic p53 peptides to the anionic DNA appeared to be facilitated by the opposing charges, it was not unexpected that the binding affinities were considerably reduced compared to the experiments done in PBS. The calculated K_d's varied between 60 and 700 mM. The complete lack of the top binding plateau made the calculations uncertain. Nevertheless, the nonphosphorylated peptide bound to the oligonucleotide stronger than the Ser378 phosphorylated peptide throughout the entire peptide concentration range. At the highest 128 mM peptide concentration the millipolarization values were 138 and 120 for the nonphosphorylated peptide and the Ser378 phosphorylated peptide, respectively. The bis-phosphorylated peptide bound to the F-trpO oligonucleotide weaker than the nonphosphorylated peptide between 4 and 32 mM and somewhat stronger between 64 and 128 mM. At this point, it cannot be unequivocally determined whether the binding differences in 50% trifluoroethanol are due to conformational alterations or bona fide affinity differences. Higher trifluoroethanol concentrations are expected to further increase the association constants and invoke additional DNA solubility problems.

Both the nonphosphorylated peptide and the Ser378 phosphorylated peptide in the Hepes buffer showed virtually identical CD spectra (Figure 5) consistent with almost entirely unordered structures. Although in our fluorescence polarization assay, both the trpO and BC-CB oligonucleotides bound to the p53 peptides, for the CD studies, we selected the latter oligonucleotide because the positive binding of a DNA sequence that is based on the BC-CB oligonucleotide probe to the C-terminal region of the full p53 protein was confirmed by independent studies earlier (*16, 32*). Mixing the Ser378 phosphorylated peptide with unlabeled BC-CB DNA fragment did not alter the CD spectrum of the phosphopeptide (Figure 5). This finding verified the direct DNA-binding experiments and indicated either that the Ser378P peptide bound to DNA very weakly or that DNA binding did not alter its structure. Mixing the unmodified peptide with the BC-CB DNA clearly reduced the intensity of the 199 nm unordered band, indicating that during these experimental conditions DNA probably bound to the peptide, and DNA binding changed the peptide conformation. Since the intensity of the unordered band was decreased after DNA binding, this conformational change likely involved the generation of a somewhat more ordered secondary structure. It needs to be mentioned that the 13% decrease in the intensity of the CD band may be due to differences in the determination of the actual peptide concentration. This possibility is unlikely, however, as after each CD had been recorded, we determined the peptide concentration carefully by RP-HPLC from the peptide solutions used for the CD analysis (*28*).

The positive binding of the nonphosphorylated and Ser378 phosphorylated peptides to the BC-CB oligonucleotide in the

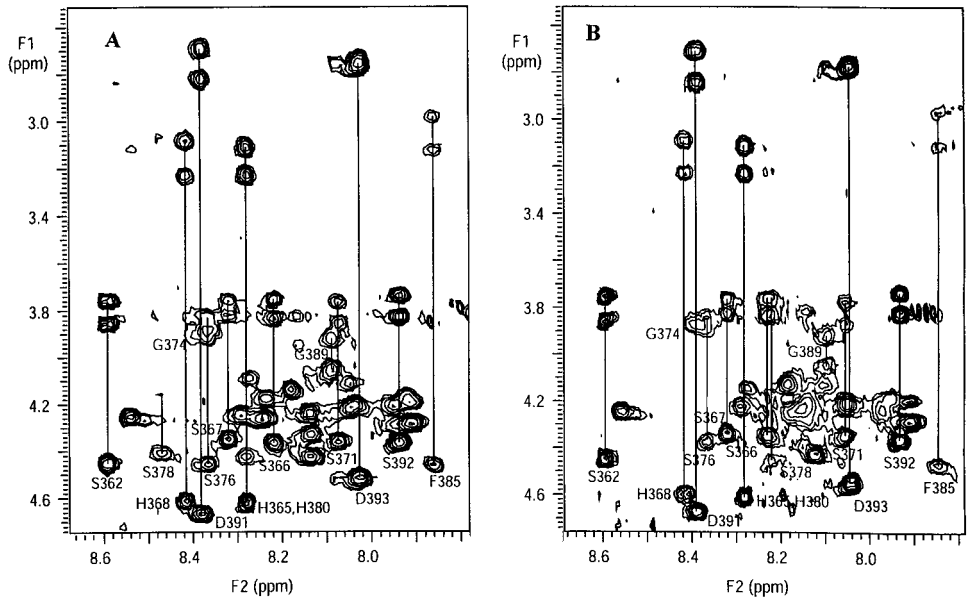

FIGURE 6: Regions of the 600 MHz TOCSY 2D spectra of (A) nonphosphorylated p53 361−393 and (B) Ser378P showing selected spin system assignments. The spectra were recorded in 50% trifluoroethanol−water at 10 °C.

Hepes−KCl buffer was verified by fluorescence polarization. We studied the binding up to 128 mM peptide concentration, which is roughly equivalent to the peptide concentration used during CD. Generally, the variability between the parallels was higher than that of other fluorescence polarization experiments. Nevertheless, it was consistent that the low to medium millimolar association constant of the nonphosphorylated peptide increased to the high mM to low millimolar range for the phosphopeptide. These findings further justified our suggestion that the nonphosphorylated peptide fragment strongly interacts with the DNA. Thus, this association may change the conformation of the C-terminal domain of p53.

NMR. A series of one-dimensional and 2D TOCSY ^{1}H NMR spectra were recorded for p53 361−393 peptide and its Ser378 phosphorylated derivative in d_3-trifluoroethanol−H_2O mixtures ranging from 50% to 100% trifluoroethanol. The spectra recorded in 50% trifluoroethanol were most suitable for analysis as they were generally the least overlapped and had the highest intensity of amide resonances. For the spectra recorded in 100% d_3-trifluoroethanol, no NH signals were visible due to exchange with deuterons of the solvent. NOESY spectra were also recorded for both peptides in 50% trifluoroethanol−50% water.

In general, the spectra were highly overlapped but were assigned using the standard sequential assignment protocol (*33*) in which resonances were first classified according to their amino acid spin systems in the TOCSY spectra and then unambiguously identified from sequential connectivities in the NOESY spectra. Figure 6 shows regions of the TOCSY spectra of both peptides and illustrates the spin system assignments. It is clear that the two peptides had very similar spectra and by implication similar conformations. Chemical shifts for both peptides are provided in Tables 3 and 4. Chemical shifts are a sensitive marker of solution conformations, and in particular, the deviations of αH shifts (see legend to Figure 7) from random coil values (secondary shifts) allow deductions about elements of secondary structure to be made (*34*). Helical structure is normally indicated by a stretch of several successive residues with negative (upfield) secondary shifts of >0.1 ppm, and extended structure is indicated by positive (downfield) secondary shifts. Figure 7 panel A shows the secondary shifts for p53 361−393 peptide and its phosphorylated derivative and in general suggests that there was a weak tendency toward helical structure for residues 381−385.

Table 3: ^{1}H-NMR Resonance Assignments of the Nonphosphorylated p53 361−393 Peptide in 50% Trifluoroethanol−H_2O at 10 °C

AA	no.	NH	α	β	γ	δ	others
gly	361		3.93				
ser	362	8.71	4.58	3.99, 2.8			
arg	363	8.68	4.38	1.94, 1.8	1.74	3.25	
ala	364	8.30	4.26	1.39			
his	365	8.40	4.74	3.36, 3.2			8.6, 7.31
ser	366	8.35	4.48	3.96, 3.8			
ser	367	8.44	4.48	3.96, 3.9			
his	368	8.54	4.73	3.36, 3.2			8.61, 7.33
leu	369	8.17	4.34	1.69	1.56	0.94, 0.9	
lys	370	8.27	4.37				
ser	371	8.18	4.48	4.0, 3.91			
lys	372	8.41	4.36				
lys	373	8.35	4.30				
gly	374	8.51	4.00				
gln	375	8.30	4.38	2.21, 2.1	2.45		
ser	376	8.49	4.50	4.02, 3.9			
thr	377	8.26	4.36	4.36	1.30		
ser	378	8.34	4.58	3.97, 3.8			
arg	379	8.30	4.25	1.88, 1.7	1.64	3.22	
his	380	8.40	4.75	3.36, 3.2			8.6, 7.31
lys	381	8.41	4.26				
lys	382	8.22	4.26				
leu	383	8.03	4.33	1.69	1.63	0.97, 0.92	
met	384	8.09	4.37	2.00	2.48, 2.4		
phe	385	7.96	4.60	3.25, 3.1			
lys	386	8.17	4.34				
thr	387	8.03	4.42	4.33	1.28		
glu	388	8.24	4.57	2.23, 2.0	2.52		
gly	389	8.22	4.18, 4.05				
pro	390		4.44	2.31, 2.0	2.05	3.69, 3.57	
asp	391	8.51	4.80	2.98, 2.8			
ser	392	8.05	4.51	3.96, 3.8			
asp	393	8.17	4.67	2.92			

Table 4: ^{1}H-NMR Resonance Assignments of the Ser378 Phosphorylated Peptide in 50% Trifluoroethanol−H_2O at 10 °C

AA	no.	NH	α	β	γ	δ	others
gly	361		3.93				
ser	362	8.71	4.58	3.99, 2.8			
arg	363	8.68	4.38	1.94, 1.8	1.74	3.25	
ala	364	8.30	4.26	1.39			
his	365	8.40	4.74	3.36, 3.2			8.6, 7.31
ser	366	8.35	4.48	3.96, 3.8			
ser	367	8.44	4.48	3.96, 3.9			
his	368	8.54	4.73	3.36, 3.2			8.61, 7.33
leu	369	8.17	4.34	1.69	1.56	0.94, 0.9	
lys	370	8.27	4.37				
ser	371	8.18	4.48	4.0, 3.91			
lys	372	8.41	4.36				
lys	373	8.35	4.30				
gly	374	8.51	4.00				
gln	375	8.30	4.38	2.21, 2.1	2.45		
ser	376	8.49	4.50	4.02, 3.9			
thr	377	8.26	4.36	4.36	1.30		
ser	378	8.34	4.58	3.97, 3.8			
arg	379	8.30	4.25	1.88, 1.7	1.64	3.22	
his	380	8.40	4.75	3.36, 3.2			8.6, 7.31
lys	381	8.41	4.26				
lys	382	8.22	4.26				
leu	383	8.03	4.33	1.69	1.63	0.97, 0.92	
met	384	8.09	4.37	2.00	2.48, 2.4		
phe	385	7.96	4.60	3.25, 3.1			
lys	386	8.17	4.34				
thr	387	8.03	4.42	4.33	1.28		
glu	388	8.24	4.57	2.23, 2.0	2.52		
gly	389	8.22	4.18, 4.05				
pro	390		4.44	2.31, 2.0	2.05	3.69, 3.57	
asp	391	8.51	4.80	2.98, 2.8			
ser	392	8.05	4.51	3.96, 3.8			
asp	393	8.17	4.67	2.92			

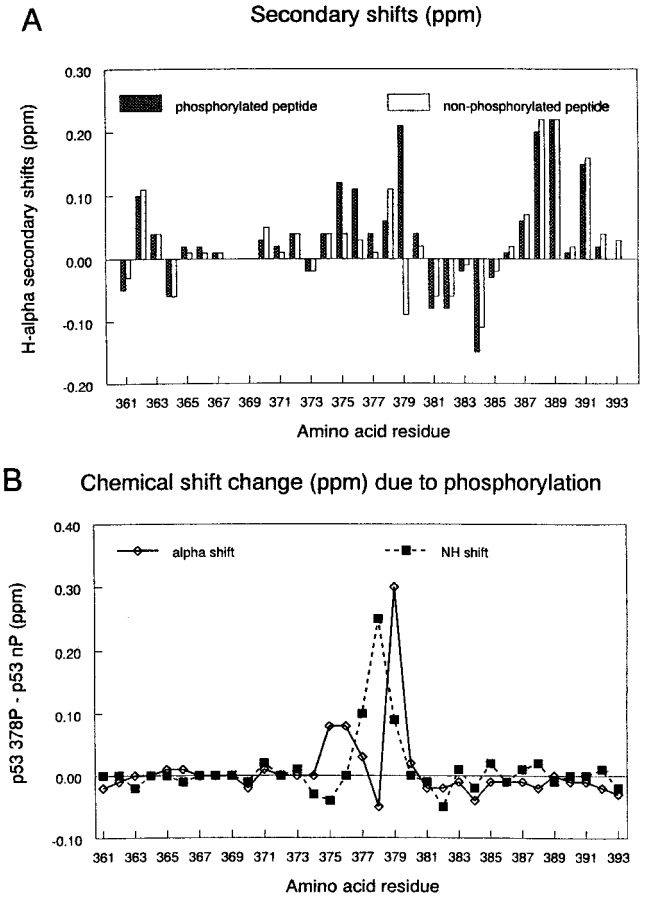

FIGURE 7: (Panel A) Secondary shifts (ppm) of nonphosphorylated p53 361−393 peptide (grey bars) and its analogue phosphorylated on Ser378 (crosshatched bars). Negative values indicate a chemical shift upfield of the random coil value of the corresponding amino acid residue, and positive values indicate downfield shifts. The random coil shifts used were those of Wishart and co-workers (*60*) for a set of peptides Gly-Gly-X-Ala-Gly-Gly recorded at pH 5.0 in deuterated buffer containing 1.0 M urea and 50 mM phosphate. These values are widely used for deduction of secondary structure in peptides and, together with the comparable data set of Merutka and co-workers (*61*), are the most recent and extensive sets of shifts available for these analyses. It was demonstrated that titration of up to 50% trifluoroethanol into aqueous solutions of random coil peptides had negligible effects on αH chemical shifts (*61*). Similarly, comparison of the data recorded at 5 °C (*61*) with those recorded at 25 °C (*60*) shows that temperature has no significant effect on αH shifts. The reported random coil values are thus suitable as reference shifts for comparison with our data in 50% aqueous trifluoroethanol at 10 °C. (Panel B) Differences in αH (open diamonds) and NH (closed squares) chemical shifts between the phosphorylated and nonphosphorylated peptides. A negative value indicates an upfield shift of the signal in the phosphorylated peptide, and the positive values indicate downfield shifts.

It is interesting that there was no difference in secondary shifts between the two peptides for the N-terminal 13 residues, but there was a small but systematic difference in the C-terminal region. This is most clearly illustrated in Figure 7 panel B which shows differences in both αH and NH shifts between the two peptides. Phosphorylation caused a significant local effect near Ser378, most notably a downfield shift of 0.25 ppm for the NH amide proton of the phosphorylated residue. There was also a general downfield shift of αH for residues flanking the phosphorylation site (i.e., 375−379). This may be the result of a simple electrostatic effect of phosphorylation, but this seems unlikely given that local effects of phosphorylation on random coil peptides are generally smaller than the effects seen here (*35*, *36*). A more likely explanation and one which is consistent with the reduction in helicity on phosphorylation detected in the CD studies is that the downfield αH shifts reflect a reduction in helicity near the phosphorylation site. Interestingly, the break in the helical structure around the phosphorylation site was compensated for by a minor increase of the helicity further down toward the C-terminus, as indicated by a very subtle upfield shift of the αH protons in the phosphorylated peptide over residues 381−393. On average, these αH protons were upfield of those in the nonphosphorylated peptide by 0.016 ppm. The effect was small, but significant, and was not simply a referencing offset as no difference in shifts was observed for the αH protons in the N-terminal region, nor for the NH protons at either the N- or C-termini (Figure 7 panel B). Because of the highly overlapped nature of the fingerprint region of the NOESY spectra, most of the medium range, i, $i + 2$ or i, $i + 3$ NOEs that would normally be used to support an interpretation of increased helicity were not unambiguously detectable. However, of the three that were not overlapped, $d_{aN}(i, i + 2)$ NOEs were detected in this region for residues 385/387 and 390/392, although not for 391/393. In addition, sequential $d_{NN}(i, i + 1)$ NOEs were detected for residues 386/387 and 387/388 in the phosphorylated peptide but not in the nonphosphorylated peptide. Thus, although most of the relevant NOE data were limited by overlap, those NOEs that were detectable supported the conclusion of mild helicity in this region.

It should be stressed that we do not suggest that the data indicate formation of a well-defined helix in this region, merely that there is a shift in the conformational equilibrium from one consisting predominantly of unordered or extended structures to one where there may be very small populations of helical forms present among the majority population of unordered or extended forms. It is interesting to speculate that the negative charge of the phosphate group, when it is placed to the N-terminal side of the helix, would interact favorably with the helix dipole (negative to positive going from the C-terminus to the N-terminus) and thus may be a driving force in the formation of these minor helical populations. According to this speculation, a longer-range effect of phosphorylation of Ser378 could be rationalized on the basis of electrostatic principles.

DISCUSSION

Published reports are contentious and contradictory on the subject of p53 binding to DNA and other related p53 functions with or without phosphorylation of the C-terminal serine residues. As for phosphorylation of Ser315 and Ser378, phosphorylation of Ser392 stimulates the sequence-specific DNA-binding activity of p53 in vitro (*15*), and this may also affect the transcriptional activity of p53 by regulating its DNA-binding affinity. Phosphorylation at Ser392 appears necessary for suppressor function since substitution with alanine abolishes the ability of p53 to suppress cell proliferation, whereas substitution with aspartic acid, which mimics phosphoserine, has only a partial effect on suppressor function (*37*). On the other hand, Fiscella et al. (*38*) reported that elimination of phosphorylation site Ser392 has no discernible effect on p53 function, and phosphorylation seems not to affect the tetramerization of p53 (*39*). Again, in contrast, most recent analyses by equilibrium ultracentrifugation showed that phosphorylation of Ser392 increases the association constant for reversible tetramer formation nearly 10-fold (*40*). The actual level of phosphorylation of the C-terminal sites is uncertain because both PKC (*41, 42*) and CKII (*43, 44*) have to be translocated from the cytosol to the nucleus to actively phosphorylate p53, possibly resulting in differences between the status of phosphorylation in healthy or cancerous cells.

A recent paper claims that individual mutations of the N-terminal serines, as well as Ser315 and Ser392 to alanine or glutamic acid, result in equivalent levels of transcriptional activation in standard transient transfection experiments (*45*). However, when p53's transcriptional activation is measured in cells that attain G1 arrest upon contact inhibition, wild-type p53 is inactive, and altering only Ser392 (and not Ser315) to glutamic acid results in a functional protein. This Ser → Glu mutant also has an increased ability to bind DNA (*45*). An assessment of the effects of phosphorylation on p53's functions by using mutated proteins is not a trivial matter because, for example, in the central core of p53, mutation of certain serine or threonine residues brings about gross conformational changes (*46*). Because the matter is so controversial, we decided to study directly the effects of phosphate incorporation on the C-terminal region of p53 by using well-characterized synthetic peptides. The peptides were thoroughly purified by RP-HPLC, and their integrity was verified by mass spectrometry eliminating the ambiguity that is inherently present when the heterogeneously phosphorylated protein is studied. The use of medium-sized synthetic peptides is justified by the domain structure of p53 and by considering that the individual domains function and fold more or less independently. The sizes of all proposed domains, except the specific DNA-binding region, are compatible with the recent technology of peptide synthesis.

Synthetic peptides were recently used to characterize the in vitro phosphorylation of murine p53 by PKC (*47*). The peptide representing the C-terminal region corresponded to amino acids 357−381; this segment is homologous to the 363−387 human sequence. PKC appears to phosphorylate the synthetic peptide at multiple Ser and Thr residues, but of the four potential sites in the murine molecule, only two are conserved in human p53. Significantly, while the nonphosphorylated murine peptide enhances sequence-specific DNA binding at millimolar concentrations, this stimulation is lost upon phosphorylation by PKC (*47*). In another recent study, a synthetic peptide corresponding to amino acids 361−382 of human p53 was shown to activate sequence-specific DNA binding of wild-type p53 in vitro, and to restore the transactivating function of at least some mutant p53 proteins in living cells (*48*).

For direct DNA-binding measurements of the human sequence, we selected fluorescence polarization because this method is performed fully in solution. Additionally, unlike methods separating the bound from the free ligand, it can provide a true equilibrium measurement of low-affinity interactions such as those between oligonucleotides and synthetic peptides. In our hands, phosphorylation at the PKC or CKII sites clearly reduced the non-sequence-specific DNA binding of the C-terminal p53 fragment. Adding a second phosphate group almost fully abolished the non-sequence-specific DNA binding. Polyclonal antibody 421 recognizes the C-terminal region of p53, and loss of the 421 epitope, through a mechanism involving increased phosphorylation at the PKC site, appears to accompany p53-mediated growth arrest (*49*). Indeed, the carboxy-terminal non-sequence-specific DNA binding is in competition with the specific DNA binding in the middle of the protein, and blocking the C-terminal domain with antibody 421 increases the sequence-specific DNA binding ability of p53 (*16*). Taken together, p53 appears to bind more strongly to DNA at the sequence-specific DNA-binding domain (amino acids 96−286) if the carboxy-terminal serines carry phosphate group(s) than if they are without phosphate.

We observed a slight conformational change in the nonphosphorylated p53 fragment when the peptide was mixed with the DNA sequence it binds to. This finding is of particular interest because it indicates that non-sequence-specific DNA binding alters the secondary structure of the basic domain, and this alteration in turn may interfere with the regular assembly of p53 mediated by the proximal tetramerization domain. The unordered secondary structure of the Ser378P peptide remained unaffected after mixing with the DNA, suggesting that the phosphopeptide−DNA interaction is weaker, fully supporting the results of the direct DNA-binding experiments. Our conclusion for the more ordered conformation of the nonphosphorylated peptide in the presence of the DNA was based on the reduction of the intensity of the unordered CD band at 199 nm. The appearance of ordered secondary structures is usually indicated by additional spectral changes. Because such

additional spectral changes were not observed, we concluded that the conformational equilibrium remained predominantly populated by irregular structures. An interesting alternative explanation for the reduced intensity of the 199 nm band is that the conformation of the oligonucleotide was changed upon binding to the nonphosphorylated peptide. This scenario, however, is unlikely. The DNA alone exhibited a classical CD spectrum characteristic for the B-form. If the reversed mathematical transaction, that is, subtraction of the peptide spectrum from the spectrum of the mixture, was made, the resulting CD curve of the DNA would be characterized by a very broad, weak, negative band between 210 and 260 nm, and a stronger, broad, positive band below 210 nm. This type of CD spectrum has not been detected so far for this family of biopolymers (*50*). The phosphorylation efficiency of p53 clearly depends on the conformation of the protein and its fragments. PKA is a potent p53 kinase and acts like all enzymes, in a conformation- and concentration-dependent manner (*51*). The dependence of the extent of phosphorylation on the conformation of p53 is further supported by the finding that the wild-type form of the protein undergoes a higher level of phosphorylation by multiple kinases in the DNA-binding domain than mutant forms of p53 (*51*).

Without addition of DNA the peptides assumed unordered conformations, in agreement with a recent study (*52*). Synthetic peptides and phosphopeptides were used to investigate the effects of phosphorylation on monomer−tetramer association and on the conformation of the C-terminal regions of p53 (*52*). As a remarkable synthetic achievement, Sakamoto and co-workers have produced 91 amino acid long peptides (amino acids 303−393) without phosphate, singly phosphorylated on Ser315, Ser378, or Ser392, and doubly phosphorylated on Ser315 and Ser392. CD in aqueous environment without organic cosolvents indicated only minor conformational differences among the nonphosphorylated Ser378 or Ser392 phosphorylated peptides.

The proximity of the basic domain and the tetramerization region also justifies the analysis of the conformation before and after phosphorylation of the basic domain without any DNA binding. Because of the frequently observed random structure of synthetic peptides in aqueous solutions, we performed the conformational analysis in trifluoroethanol and trifluoroethanol−water mixtures, solvent systems with proven applicability for peptide structural analysis (*30*). Trifluoroethanol, like many other alcohols, is a structure stabilizing/inducing solvent (*53*, *54*) that is extensively used to mimic the dynamic hydrophobic−hydrophilic environment of the cells (*55*, *56*) since the cell milieu is not nearly as polar as pure water (*57*). We attempted to qualitatively correlate the effect of phosphorylation on the conformation of the p53 peptides in trifluoroethanol−water mixtures with the effect on DNA binding. Phosphate incorporation into Ser378 reduced peptide helicity around this residue, and addition of phosphate to Ser392 further enhanced this effect. On the same token, the nonphosphorylated peptide bound to the F-trpO oligonucleotide stronger than the Ser378 phosphorylated peptide in both PBS and a trifluoroethanol−PBS = 1:1 (v/v) mixture. On the basis of these experiments alone, it cannot be resolved whether the decrease of the DNA binding of the phosphopeptides is due to phosphate incorporation per se or reflects conformation-related effects. At the full protein level, however, the conformational changes after phosphorylation and diminished non-sequence-specific DNA binding may go hand in hand. On the basis of our results it is tempting to speculate that phosphorylation at the C-terminal domain regulates the tetramerization process of the full protein.

The NMR data suggested that in 50% trifluoroethanol both peptides were generally unordered except for nascent helical structure near residues 381−385. The helical tendency around the PKC site was slightly decreased and further downstream was slightly increased by phosphorylation. The NMR results are complementary to the CD findings in that they allow the location of conformational changes to be determined rather than just information on helical content. NMR spectra recorded at increasing trifluoroethanol concentrations showed an upfield shift of the αH resonances, consistent with the CD finding of increasing helical content with increasing trifluoroethanol. A direct comparison of the NMR and CD data in 100% trifluoroethanol was not possible because of the difficulty in assigning the NMR spectra in 100% trifluoroethanol (as noted above, these spectra had no NH signals). However, it is interesting to compare the two techniques in terms of their detection of the effects of phosphorylation on helicity. In 100% trifluoroethanol, the CD data suggest that phosphorylation slightly reduces the overall helix content. The NMR data presented above for 50% trifluoroethanol show a somewhat increased helical tendency in the C-terminal third of the molecule upon phosphorylation. This is not inconsistent with the CD data though, as the NMR data, also show a more significant increase in extended structure near Ser378 on phosphorylation. CD effectively monitors the sum of the two conformational effects, while NMR highlights the two opposing trends at different locations.

Our synthetic peptides and phosphopeptides will be useful for studying two additional characteristic and important functions of p53: antibody binding and turnover. Phosphorylation of the PKC site is reported to inhibit the recognition by antibody 421 (*50*), although the loss of 421 activity in EB-1 cells can be correlated with glycosylation in the epitope region (*58*). Our preliminary results indicated that the Ser378 phosphorylated peptide was recognized much less efficiently than the nonphosphorylated parent analogue, but because antibody 421 bound weakly to the peptides (*59*), this finding needs to be treated with caution. The synthetic phosphopeptides as immunogens are, however, promising candidates to generate phosphorylation-specific monoclonal antibodies.

ACKNOWLEDGMENT

The authors wish to thank Dr. Magda Thurin for critical reading of the manuscript, Dr. Thanos Halazonetis for recombinant p53 and antibody 421, Istvan Varga for technical help, and Shirley Peterson, Anne Marie Pease, and Jennifer R. Levicke for editorial help. D.J.C. is an Australian Research Council Professorial Fellow.

REFERENCES

1. Lane, D. P. (1992) *Nature 358*, 15−16.
2. Hollstein, M., Sidransky, D., Vogelstein, B., and Harris, C. C. (1991) *Science 253*, 49−53.
3. Jenkins, J. R., Rudge, K., and Currie, G. A. (1984) *Nature 312*, 651−654.

4. Rovinski, B., and Benchimol, S. (1988) *Oncogene 2*, 445−452.
5. Donehower, L. A., and Bradley, A. (1993) *Biochim. Biophys. Acta 1155*, 181−205.
6. Ko, L. J., and Prives, V. (1996) *Genes Dev. 10*, 1054−1072.
7. Walker, K. H., and Levine, A. J. (1996) *Proc. Natl. Acad. Sci. U.S.A. 93*, 15335−15340.
8. Fields, S., and Jang, S. K. (1990) *Science 249*, 1046−1049.
9. Cho, J., Gorina, S., Jeffrey, P. D., and Pavletich, N. P. (1994) *Science 265*, 346−355.
10. Sakamoto, H., Lewis, M. S., Kodama, H., Appella, E., and Sakaguchi, K. (1994) *Proc. Natl. Acad. Sci. U.S.A. 91*, 8974−8978.
11. Clore, G. M., Omichinski, J. G., Sakaguchi, K., Zambrano, N., Sakamoto, H., Appella, E., and Gronenborn, A. M. (1995) *Science 265*, 386−391.
12. Clubb, R. T., Omichinski, J. G., Sakaguchi, K., Appella, E., Gronenborn, A. M., and Clore, G. M. (1995) *Protein Sci. 4*, 855−862.
13. Buchman, V. L., Chumakov, P. M., Ninkina, N. N., Samarina, O. P., and Georgiev, G. P. (1988) *Gene 70*, 245−252.
14. Farrel, P. J., Allan, G. J., Shanahan, F., Vousden, K. H., and Crook, T. (1991) *EMBO J. 10*, 2879−2887.
15. Hupp, T. R., Meek, D. W., Midgley, C. A., and Lane, D. P. (1992) *Cell 71*, 875−886.
16. Bayle, J. H., Elenbaas, B., and Levine, A. J. (1995) *Proc. Natl. Acad. Sci. U.S.A. 92*, 5729−5733.
17. Jayaraman, L., and Prives, C. (1995) *Cell 81*, 1021−1029.
18. Lee, S., Elenbaas, B., Levine, A., and Griffith, J. (1995) *Cell 81*, 1013−1020.
19. Baudier, J., Delphin, C., Grunwald, D., Khochbin, S., and Lawrence, J. L. (1992) *Proc. Natl. Acad. Sci. U.S.A. 89*, 11627−11631.
20. Takenaka, I., Morin, F., Seizinger, B. R., and Kley, N. (1995) *J. Biol Chem. 270*, 5405−5411.
21. Meek, D. W., Simon, S., Kikkawa, U., and Eckhart, W. (1990) *EMBO J. 9*, 3253−3260.
22. Herrmann, C. P., Kraiss, S., and Montenarh, M. (1991) *Oncogene 6*, 877−884.
23. Fields, G. B., and Noble, R. L. (1990) *Int. J. Pept. Protein Res. 35*, 161−214.
24. Wakamiya, T., Saruta, K., Yasuoka, J., and Kusumoto, S. (1994) *Chem. Lett.* 1099−1102.
25. Yonemoto, W., McGlone, M. L., Grant, B., and Taylor, S. (1997) *Protein Eng. 8*, 915−925.
26. Lundblad, J. R., Laurance, M., and Goodman, R. H. (1996) *Mol. Endocrinol. 10*, 607−612.
27. LeTilly, V., and Royer, C. A. (1993) *Biochemistry 32*, 7753−7758.
28. Szendrei, G. I., Fabian, H., Mantsch, H. H., Lovas, S., Nyeki, O., Schon, I., and Otvos, L., Jr. (1994) *Eur. J. Biochem. 226*, 917−924.
29. Woody, R. W. (1985) in *The peptides* (Hruby, V. J., Ed.) pp 15−114, Academic Press, Orlando, FL.
30. Otvos, L., Jr. (1996) in *Neuropeptide Protocols* (Irvine, G. B., andWilliams, C. H., Eds.) pp 153−161, Humana Press, Totowa, NJ.
31. Greenfield, N., and Fasman, G. D. (1969) *Biochemistry 8*, 4108−4116.
32. Halazonetis, T. D., and Kandil, A. N. (1993) *EMBO J. 12*, 5057−5064.
33. Wuthrich, K. (1986) *NMR of Proteins and Nucleic Acids*, Wiley, New York.
34. Wishart, D. S., Sykes, B. D., and Richards, F. M. (1992) *Biochemistry 31*, 1647−1651.
35. Hoffmann, R., Reichert, I., Wachs, W. O., Zeppezauer, M., and Kalbritzer, H. R. (1994) *Pept. Protein Res. 44*, 193−198.
36. Quirk, P. G., Patchell, V. B., Colyer, J., Drago, G. A., and Gao, Y. (1996) *Eur. J. Biochem. 236*, 85−91.
37. Milne, D. M., Palmer, R. H., and Meek, D. W. (1992) *Nucleic Acids Res. 20*, 5565−5570.
38. Fiscella, M., Zambrano, N., Ullrich, S. J., Unger, T., Lin, D., Cho, B., Mercer, W. E., Anderson, C. W., and Appella, E. (1994) *Oncogene 9*, 3249−3257.
39. Roley, N., and Milner, J. (1994) *Oncogene 9*, 3067−3070.
40. Sakaguchi, K., Sakamoto, H., Lewis, M. S., Anderson, C. W., Erickson, J. W., Appella, E., and Xie, D. (1997) *Biochemistry 36*, 10117−10124.
41. Leach, K. L., and Raben, D. M. (1993) *Biochem. Soc. Trans 21*, 879−883.
42. Simboli-Campbell, M., Gagnon, A., Franks, D. J., and Welsh, J. (1994) *J. Biol. Chem. 269*, 3257−3264.
43. Filhol, O., Loue-Mackenbach, P., Cochet, C., and Chambaz E. M. (1991) *Biochem. Biophys. Res. Commun. 180*, 623−630.
44. Lorenz, P., Pepperkok, R., Ansorge, W., and Pyerin, W. (1993) *J. Biol. Chem. 268*, 2733−2739.
45. Hao, M., Lowy, A. M., Kapoor, M., Deffie, A., Liu, G., and Lozano, G. (1996) *J. Biol. Chem. 271*, 29380−29385.
46. Milne, D. M., McKendrick, L., Jardine, L. J., Deacon, E., Lord, J. M., and Meek, D. W. (1996) *Oncogene 13*, 205−211.
47. Delphin, C., Huang, K.-P., Scotto, C., Chapel, A., Vincon, M., Chambaz, E., Garin, J., and Baudier, J. (1997) *Eur. J. Biochem. 245*, 684−692.
48. Selivanova, G., Iotsova, V., Okan, I., Fritzsche, M., Strom, M., Gorner, B., Galfstrom, R. C., and Wilman, K. G. (1997) *Nature Med. 3*, 632−638.
49. Ullrich, S. J., Mercer, W. E., and Appella, E. (1992) *Oncogene 7*, 1635−1643.
50. Johnson, W. C. (1994) in *Circular Dichroism: Principles and Applications* (Nakanishi, K., Berova, N., and Woody, R. W., Eds.) pp 523−540, VCH Publishing, New York.
51. Adler, V., Pincus, M. R., Minamoto, T., Fuchs, S. Y., Bluth, M. J., Brandt-Rauf, P. W., Friedman, F. K., Robinson, R. C., Chen, J. M., Wang, X. W., Harris, C. C., and Ronai, Z. (1997) *Proc. Natl. Acad. Sci. U.S.A. 94*, 1686−1691.
52. Sakamoto, H., Kodama, H., Higashimoto, Y., Kondo, M., Lewis, M. S., Anderson, C. W., Appella, E., and Sakaguchi, K. (1996) *Int. J. Pept. Protein Res. 48*, 429−442.
53. Conio, G., Patrone, E., and Brighetti, S. (1970) *J. Biol. Chem. 245*, 3335−3340.
54. Nelson, J. W., and Kallenbach, N. R. (1986) *Proteins 1*, 211−217.
55. Urry, D. W., Masotti, L., and Krivacic, J. R. (1971) *Biochim. Biophys. Acta 241*, 600−612.
56. Otvos, L., Jr., Szendrei, G. I., Lee, V. M.-Y., and Mantsch, H. H. (1993) *Eur. J. Biochem. 211*, 249−257.
57. Lehrmann, S. R., Tuls, J. L., and Lund, M. (1990) *Biochemistry 29*, 5590−5596.
58. Shaw, P., Freeman, J., Bovey, R., and Iggo, R. (1996) *Oncogene 12*, 921−930.
59. Hoffmann, R., Bolger, R. E., Xiang, Z. Q., Blaszczyk-Thurin, M., Ertl, H. C. J., and Otvos, L., Jr. (1998) in *Peptides: Chemistry, Structure and Biology* (Tam, J. P., and Kaumaya, P. T. P., Eds.) Kluwer (in press).
60. Wishart, D. S., Bigam, C. G., Holm, A., Hodges, R. S., and Sykes, B. D. (1995) *J. Biomol. NMR 5*, 67−81.
61. Merutka, G., Dyson, H. J., and Wright, P. E. (1995) *J. Biomol. NMR 5*, 14−24.

BI980760A